Geochemistry Geophysics Geosystems G3

Published by AGU and the Geochemical Society

Article
Volume 00, Number 00
0 MONTH 2013
doi: 10.1002/ggge.20198
ISSN: 1525-2027

Film drainage and the lifetime of bubbles

C. T. Nguyen, H. M. Gonnermann, and Y. Chen
Department of Earth Science, Rice University, Houston, Texas, 77005, USA (ctn2@rice.edu)

C. Huber
School of Earth and Atmospheric Sciences, Georgia Institute of Technology, Atlanta, Georgia, USA

A. A. Maiorano and A. Gouldstone
Department of Mechanical and Industrial Engineering, Northeastern University, Boston, Massachusetts, USA

J. Dufek
School of Earth and Atmospheric Sciences, Georgia Institute of Technology, Atlanta, Georgia, USA

[1] We present the results of new laboratory experiments that provide constraints on inter bubble film thinning and bubble coalescence as a consequence of liquid expulsion by gravitational and capillary forces. To ensure dynamic similarity to magmatic systems, the experiments are at small Reynolds numbers ($Re \ll 1$) and cover a wide range of Bond numbers ($10^{-3} \leq Bo \leq 10^{2}$). Results indicate that at $Bo < 0.25$ film drainage is due to capillary forces, whereas at $Bo > 0.25$ gravitational forces result in film thinning. The film drainage time scale is given by $t \sim C \ln(\alpha)\, \tau$ and is orders of magnitude faster than often assumed for magmatic systems. Here, $C \sim 10$ is an empirical constant and α is the ratio of initial film thickness to film thickness at the time of rupture and τ is the characteristic capillary or buoyancy time scale at values of $Bo < 0.25$ and $Bo > 0.25$, respectively.

Components: 13,295 words, 9 figures, 1 table.

Keywords: film drainage; bubble coalescence; bubble lifetime; volcanic eruptions; magmatic processes; volcanology.

Index Terms: 8450 Planetary volcanism: Volcanology; 8428 Explosive volcanism: Volcanology; 8430 Volcanic gases: Volcanology; 8445 Experimental volcanism: Volcanology; 6063 Volcanism: Planetary Sciences: Comets and Small Bodies; 8148 Planetary volcanism: Tectonophysics; 4302 Geological: Natural Hazards; 5480 Volcanism: Planetary Sciences: Solid Surface Planets.

Received 10 April 2013; **Revised** 4 June 2013; **Accepted** 7 June 2013; **Published** 00 Month 2013.

Nguyen, C. T., H. M. Gonnermann, Y. Chen, C. Huber, A. A. Maiorano, A. Gouldstone, and J. Dufek (2013), Film drainage and the lifetime of bubbles, *Geochem. Geophys. Geosyst.*, *14*, doi:10.1002/ggge.20198.

1. Introduction

[2] Magmatic processes that govern explosive volcanic eruptions are largely inaccessible to direct observation. To reconstruct the subsurface processes that determine eruptive style and intensity, scientists rely on indirect observations and direct observations from eruptive products that are pyroclasts. Of fundamental importance for volcanic eruptions are magmatic volatiles and their exsolution because they affect magma buoyancy [e.g., *Gonnermann and Manga*, 2007], magma rheology [e.g., *Stein and Spera*, 1992; *Manga et al.*, 1998; *Rust and Manga*, 2002; *Pal*, 2003; *Llewellin and*

Manga, 2005], as well as the potential energy required for explosive eruptive behaviors [e.g., *Sparks*, 1978; *Alidibirov and Dingwell*, 2000; *Spieler et al*., 2004; *Koyaguchi and Mitani*, 2005; *Namiki and Manga*, 2005; *Mueller et al*., 2008; *Koyaguchi et al*., 2008; *Namiki and Manga*, 2008; *Alatorre-Ibargüengoitia et al*., 2010].

[3] Volatile exsolution results in the formation of bubbles within the ascending magma, which may become preserved as vesicles in pyroclasts. Fundamental properties of pyroclasts are therefore the volume fraction of vesicles and their size distribution [e.g., *Sparks*, 1978; *Sparks and Brazier*, 1982; *Whitham and Sparks*, 1986; *Houghton and Wilson*, 1989; *Toramaru*, 1989, 1990; *Cashman and Mangan*, 1994; *Blower et al*., 2003; *Burgisser and Gardner*, 2005]. They are thought to provide fundamental constraints on the magma vesiculation process and by inference on magma ascent rates and dynamics [e.g., *Rutherford and Hill*, 1993; *Lovejoy et al*., 2004; *Gaonac'h et al*., 2005; *Toramaru*, 2006; *Blundy and Cashman*, 2008; *Rutherford*, 2008; *Gonnermann and Houghton*, 2012]. Vesicle volume fraction and size distribution are thought to provide a time-integrated record of syneruptive bubble nucleation, bubble growth, bubble coalescence, and open-system degassing through permeable bubble networks that are formed by bubble coalescence [e.g., *Eichelberger et al*., 1986; *Westrich and Eichelberger*, 1994; *Klug and Cashman*, 1996; *Saar and Manga*, 1999; *Blower*, 2001; *Burgisser and Gardner*, 2005; *Okumura et al*., 2006; *Wright et al*., 2006; *Namiki and Manga*, 2008; *Okumura et al*., 2008; *Wright et al*., 2009; *Rust and Cashman*, 2011; *Castro et al*., 2012].

[4] Of these three processes—nucleation, growth, and coalescence—bubble coalescence is perhaps the most difficult one to reconstruct quantitatively from vesicle size distributions, in part because of a relative dearth of rigorous quantitative constraints on coalescence rates [e.g., *Herd and Pinkerton*, 1997; *Klug and Cashman*, 1996; *Klug et al*., 2002; *Lovejoy et al*., 2004; *Gaonac'h et al*., 2005; *Burgisser and Gardner*, 2005; *Gardner*, 2007; *Bai et al*., 2008; *Gonde et al*., 2011; *Castro et al*., 2012]. Not only is this of importance for the eruptive process itself, but also to assess the extent to which vesicles record bubble coalescence during the time interval between pyroclast formation by magma fragmentation and quenching.

[5] The objective of this study is to provide some new constraints on bubble coalescence rates. Coalescence is the process whereby the liquid film that separates adjacent bubbles thins and ruptures, transforming two or more individual bubbles into a single bubble of larger size [*Chan et al*., 2011, and references therein]. Because coalescence is a consequence of thinning of the liquid film that separates bubbles, the rates of film thinning under different conditions of driving and resisting forces provide a fundamental constraint on bubble coalescence rates and will be the focus of our study.

[6] Film thinning can be caused by liquid expulsion due to (1) gravitational forces, associated with the density difference between bubbles and surrounding liquid [e.g., *Jones and Wilson*, 1978; *Proussevitch et al*., 1993; *Debrégeas et al*., 1998]; (2) capillary forces [e.g., *Proussevitch et al*., 1993]; (3) bubble growth, due to decompression or diffusion of dissolved gases from the liquid to bubbles [e.g., *Gardner*, 2007]; as well as (4) shearing induced by the flow of the entire suspension, for example, during magma ascent [e.g., *Okumura et al*., 2006, 2008; *Castro et al*., 2012], or perhaps induced by bubble coalescence itself [e.g., *Martula et al*., 2000].

[7] Here, we present new results of laboratory experiments on film drainage of "bare" viscous bubbles [*Debrégeas et al*., 1998], as a consequence of liquid expulsion (drainage) by both gravitational and capillary forces. The results of our experiments provide a base case against which experiments or predictions of bubble coalescence in more complicated cases, for example, those involving multiple bubbles or growing bubbles, can be compared. Figure 1 illustrates the analogy between such film drainage in experiments and vesicular magmas, as preserved in pyroclasts. We refer the reader to section 2 for a general introduction to film drainage and to section 3 for a detailed discussion of our experiments, including the similarity between film drainage in our experiments and in magmas. We discuss our experimental results in section 4 and provide a brief discussion of potential applications of our results to magmatic systems in section 5.

2. Film Drainage

2.1. Previous Work

[8] The drainage of liquid films has been studied extensively [e.g., *Charles and Mason*, 1960; *Princen*, 1963; *Hartland*, 1970]. In our experiments, the film was the surfactant-free liquid layer surrounding a stationary air bubble suspended

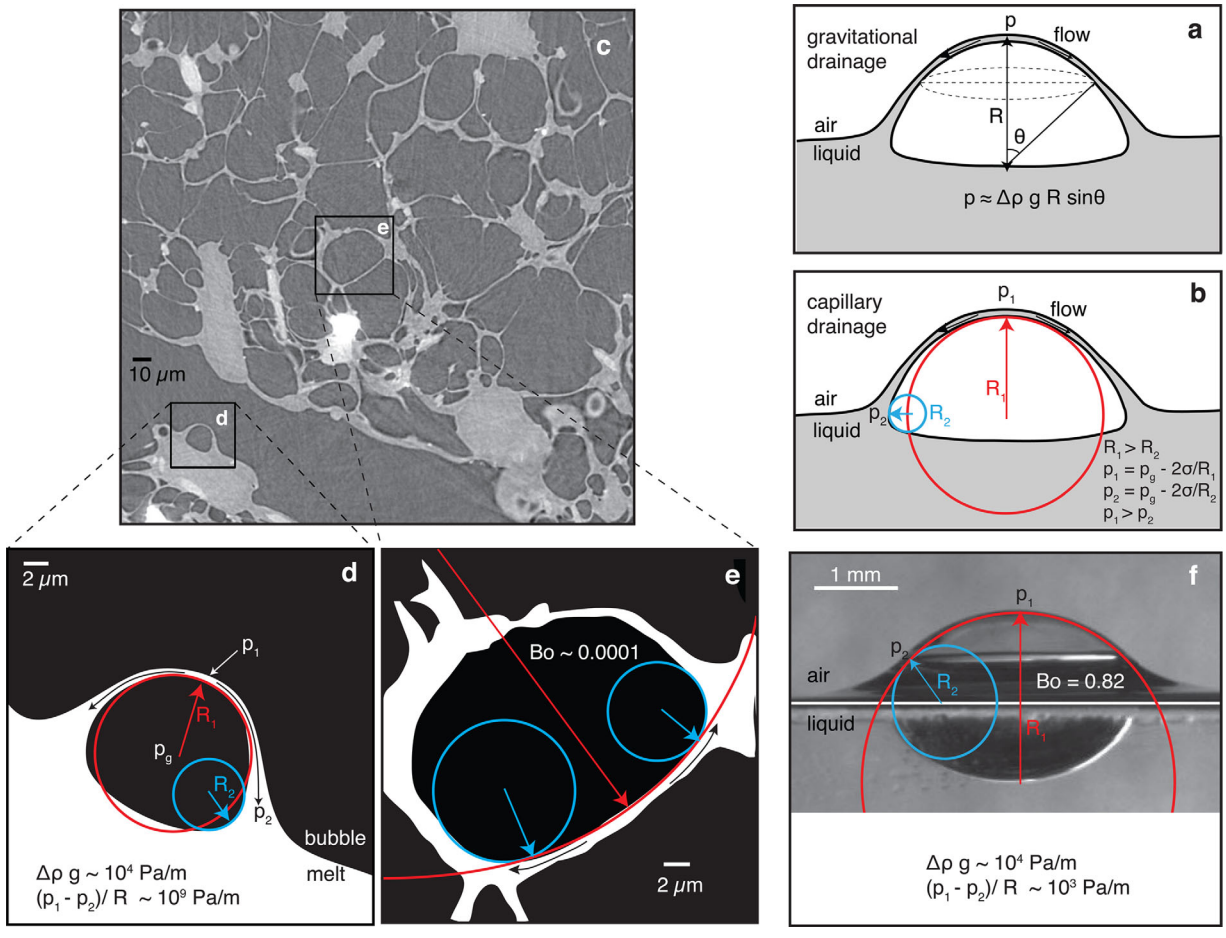

Figure 1. Film drainage in vesicular magma and laboratory experiments. Schematic diagram of a bubble and surrounding liquid, illustrating (a) gravitational and (b) capillary film drainage. (c) A CT-scan image of Soufrière Hills pumice sample PV3–800 × 800-504 showing vesicular texture with thin interbubble films (courtesy of T. Giachetti and discussed in *Giachetti et al.* [2011]). The vesicles presumably preserve the shapes, sizes, and distribution of bubbles within the pyroclast prior to quenching. (d and e) Individual vesicles at higher magnification and with annotation to highlight the change in curvature along the melt film. Also indicated are estimates of the ensuing capillary pressure gradient that would have driven film drainage, $(p_2 - p_1)/R \sim 10^9$ Pa m^{-1}, for a constant pressure p_g inside the bubble and bubble radius, R. The pressure gradient due to gravity is $\Delta\rho g \sim 10^4$ Pa m^{-1}, where $\Delta\rho$ denotes the difference in density between liquid and bubble and g is the acceleration due to gravity. (f) Example of a bubble from one of our film drainage experiments, showing the change in curvature along the melt film surrounding the bubble, as well as estimated difference in pressure due to surface tension at $\sim 10^3$ Pa m^{-1}. The pressure gradient due to gravity is $\Delta\rho g \sim 10^4$ Pa m^{-1}. Regardless of precise geometry that is multiple bubbles in magma at some orientation or a single bubble in our experiment, gravity, and changes in the radius of curvature result in pressure gradients within the film that drive film drainage. Depending on bubble size, the relative magnitude of these driving forces changes, as quantified by the Bond number.

beneath the free surface of a liquid layer. Formulations for the variation in film thickness, δ, with time, t, have been derived from lubrication theory under the assumption of immobile interfaces, that is no-slip boundaries on either side of the liquid film (Figure 2a) [e.g., *Charles and Mason*, 1960; *Hartland*, 1970; *Ivanov and Traykov*, 1976; *Toramaru*, 1988; *Proussevitch et al.*, 1993]

$$t \sim \frac{3n^2}{16\pi}\frac{\eta A^2}{F}\left(\frac{1}{\delta^2} - \frac{1}{\delta_0^2}\right). \quad (1)$$

[9] Here, $\delta = \delta_0$ when $t = 0$, $A \approx \pi R^2$ is the area of the draining film, R is the bubble radius, and η is the liquid viscosity. F is the force, either gravitational or capillary, acting on the drop and causing film drainage, and n is the number of immobile film interfaces.

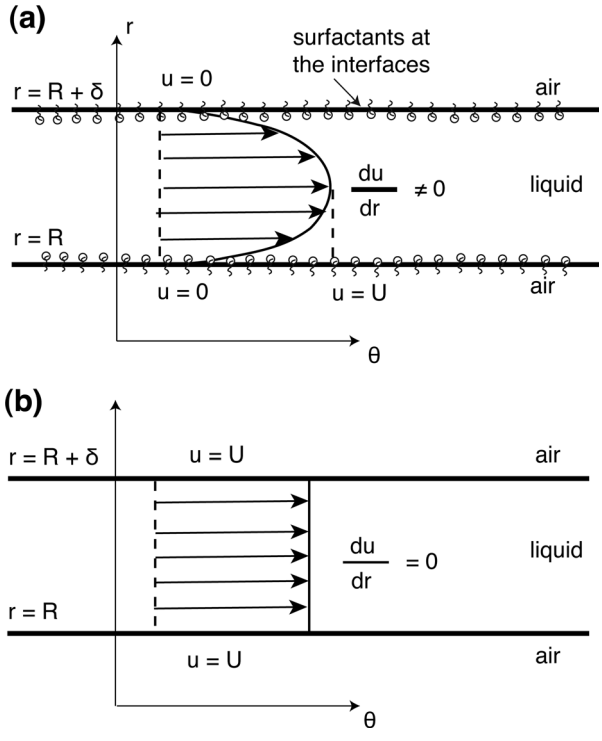

Figure 2. Schematic diagrams illustrating the mobility of gas-liquid interfaces: (a) The velocity profile for flow in a film with immobile interfaces and (b) the velocity profile for fully mobile interfaces.

[10] For $n = 2$, a strongly stabilizing surfactant layer or other impurities cause both sides of the liquid film to be immobile. The velocity of the liquid within the film approaches zero at the interfaces and the resultant flow approximates to a Hagen-Poiseuille velocity profile [e.g., *Lee and Hodgson*, 1968]. In the absence of surfactants or other impurities that may change the film interfaces from being a completely free-slip boundary, it is expected that $n \ll 2$ [*Hartland*, 1970]. In this case, the flow within the film should be a plug flow (Figure 2b) [e.g., *Lee and Hodgson*, 1968]. In practice, many applications may involve partially mobile interfaces [e.g., *Chesters and Hofman*, 1982; *Chesters*, 1988; *Yiantsios and Davis*, 1991; *Abid and Chesters*, 1994; *Oldenziel et al.*, 2012] with some intermediate value of n in the range of $0 < n < 2$.

[11] Precise values of n for bubbles in magmas, where the film interfaces may not be immobile, do not exist and it has typically been assumed that $n = 2$ [*Toramaru*, 1988; *Proussevitch et al.*, 1993; *Klug et al.*, 2002; *Cashman and Mangan*, 1994; *Klug and Cashman*, 1996; *Mangan and Cashman*, 1996; *Cruz and Chouet*, 1997; *Navon and Lyakhovsky*, 1998; *Castro et al.*, 2012]. We will see subsequently that this can result in significant inaccuracies of estimated film drainage times.

2.2. The Capillary Length

[12] If $R \ll \sqrt{\sigma/\Delta\rho g}$, film drainage and bubble coalescence (neglecting bubble growth and deformation) are expected to be a consequence of capillary film drainage, with $F = 2\pi\sigma A/R$. Here, $\Delta\rho$ is the density difference between bubble and surrounding liquid, g is the acceleration due to gravity, and σ is surface tension.

[13] In contrast, for $R \gg \sqrt{\sigma/\Delta\rho g}$, gravitational drainage is expected to dominate and $F = 4\pi R^3 \Delta\rho g/3$ [e.g., *Charles and Mason*, 1960; *Hartland*, 1970]. The length scale

$$\lambda = \sqrt{\sigma/\Delta\rho g} \tag{2}$$

is called the capillary length and for bubbles in silicate melts it is thought to be of the order of 1 mm [*Proussevitch et al.*, 1993].

2.3. Gravitational Drainage of "Bare" Viscous Bubbles

[14] Consistent with previous results [*Debrégeas et al.*, 1998; *van der Schaaf and Beerkens*, 2006], we find that in the absence of any surfactants or impurities, equation (1) does not reproduce the experimentally observed rates of gravitational film drainage, even for very small values of n [e.g., *Davis and Smith*, 1976; *Traykov et al.*, 1977].

[15] An alternate equation for the lifetime of such "bare" viscous bubbles, where films are not protected by surfactants or impurities, is based on fully mobile film interfaces [*Debrégeas et al.*, 1998; *van der Schaaf and Beerkens*, 2006]. Consider a buoyant bubble of radius R, surrounded by a liquid film beneath a free surface (Figure 1a). Assuming a longitudinally uniform film thickness $(\partial\delta/\partial\phi = 0)$ and velocity within the film $(\partial u/\partial\phi = 0)$, an equation for the drainage velocity is given by

$$u(\theta) = c(\theta)\frac{1}{\eta}\Delta\rho g R^2, \tag{3}$$

where c is a parameter that depends on the latitudinal position θ and the driving force for film drainage is given by $F = 4\pi R^3 \Delta\rho g/3$.

[16] Local mass conservation, assuming that the liquid is incompressible, leads to

$$\frac{1}{R}\frac{\partial(\delta u)}{\partial\theta}+\frac{\partial\delta}{\partial t}=0, \tag{4}$$

where δ is the film thickness. Substituting equation (3) in the continuity equation leads to

$$\left.\frac{d\delta}{dt}\right|_{\theta=0}=-\frac{1}{C_g}\frac{\delta\Delta\rho gR}{\eta}, \tag{5}$$

where $u=0$ at $\theta=0$. Integration with separation of variables [*Debrégeas et al.*, 1998; *van der Schaaf and Beerkens*, 2006] results in

$$t_g=C_g\ln\left(\frac{\delta_0}{\delta_f}\right)\underbrace{\frac{\eta}{\Delta\rho gR}}_{\tau_g}. \tag{6}$$

[17] Here, t_g is the time required for gravitational film drainage at the apex of the bubble from an initial thickness, δ_0, to a final thickness, δ_f, at which spontaneous rupture occurs. $\tau_g=\eta/(\Delta\rho gR)$ is the characteristic buoyancy time scale and C_g is an empirical constant.

2.4. Capillary Drainage of "Bare" Viscous Bubbles

[18] In magmas, bubble sizes may range over many orders of magnitude, often with $R\ll\lambda$. In the absence of bubble growth, coalescence at $R<\lambda$ is a consequence of capillary film drainage (Figure 1b), which is not well constrained by experiments, because of the difficulty of working with bubbles at the required small values of R and Bo (see section 3.2.3). Here, we show that the general form of equation (6) also applies for film drainage of bare viscous bubbles at $R\ll\lambda$.

[19] Using a similar approach to the derivation of equation (6), we obtain for the velocity of the melt film

$$u(\theta)=c(\theta)\frac{1}{\eta}\sigma, \tag{7}$$

where the driving force that generates the flow is due to surface tension, $F=2\sigma A/R$, and spans two orders of magnitude in our experiments. Using the continuity equation for mass balance along θ, that is equation (4), we obtain

$$\left.\frac{\mathrm{d}\delta}{\mathrm{d}t}\right|_{\theta=0}=-\frac{1}{C_c}\frac{\delta\sigma}{\eta R}. \tag{8}$$

[20] From integration by separation of variables, the capillary film drainage time is obtained as

$$t_c=C_c\ln\left(\frac{\delta_0}{\delta_f}\right)\underbrace{\frac{\eta R}{\sigma}}_{\tau_c}, \tag{9}$$

where $\tau_c=\eta R/\sigma$ is the characteristic capillary time scale and C_c is an empirical constant.

3. Experiments

3.1. Overview

[21] We performed experiments in which a bubble of laboratory air was injected at the bottom of a layer of polydimethylsiloxane melt (PDMS a.k.a. silicone oil) and rose to the free surface. In our experiments, the width of the experimental box was always at least five times larger than the bubble diameter to avoid any boundary effects. During the experiments, bubble motion underwent two stages. The first stage was the buoyant ascent of the bubble toward the interface and the second was the drainage of the interfacial film above the stationary bubble [*Pigeonneau and Sellier*, 2011]. Once the bubble approached the surface, its rise velocity rapidly decreased, forming a protruding hemispherical cap of radius, $R_{\mathrm{cap}}\sim R=(3V/4\pi)^{1/3}$, where V is the volume of the bubble. Subsequently during the second stage, the liquid film that formed the cap thinned from an initial thickness, δ_0, to a thickness, δ_f, at which the bubble spontaneously ruptured (Figures 3 and 4). The whole process was captured at up to 80 frames per second using a charge-coupled device camera connected to a Zeiss SteREO® microscope. The captured images were analyzed to measure bubble dimensions, as well as the time elapsed during stage two, that is between when the bubble rise velocity became negligible and when the bubble spontaneously ruptured (Figure 3). This duration is herein defined as drainage time, t_d, and corresponds to a change of film thickness from $\delta_0\sim 100$ μm to $\delta_f\sim 100$ nm, or $\ln(\delta_0/\delta_f)\approx 7$.

3.2. Dynamic Similarity

[22] Dynamic experiments on silicate melts are complicated, due in part to the requirement for high temperatures. To overcome this and other difficulties, analogue materials are commonly used in the study of magmatic processes [*Mader et al.*, 2004]. However, for any laboratory experiment to provide useful constraints on the natural system, careful consideration must be given to appropriate scaling of laboratory conditions with respect to the natural processes in question.

[23] Two fluid-dynamical processes are considered to be dynamically similar, if the ratios of all forces

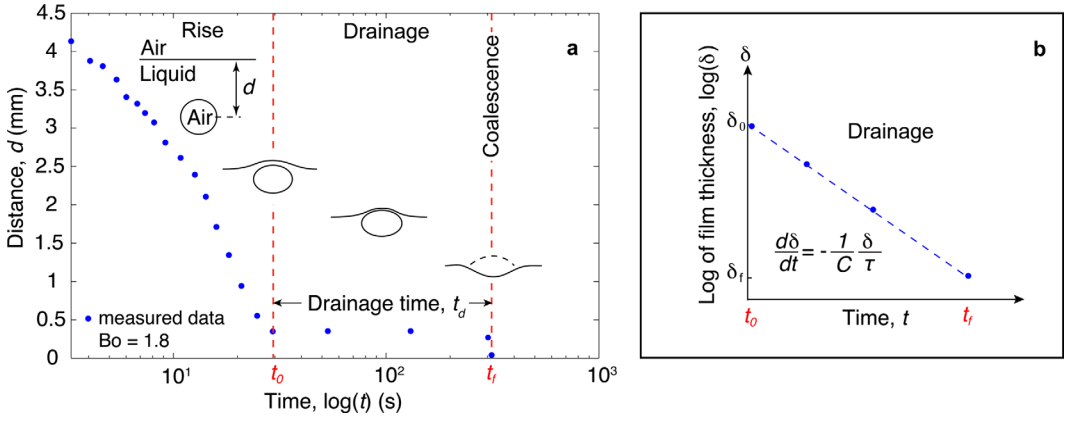

Figure 3. (a) A typical experiment, showing measured position of the bubble relative to the free surface, d. As the bubble approaches the free surface its velocity decreases. Once the bubble rise velocity approaches zero, film drainage begins and the drainage time, t_d, is defined as the time thereafter until the bubble ruptures. (b) Schematic diagram of film thinning, with the constant film thinning rate $d\delta/dt$ in semilog scale, indicating that film thickness decays exponentially with time.

acting on corresponding fluid volumes and surfaces in the two systems are the same [*Kline*, 1986]. This can be achieved rigorously through dimensional analysis, which permits the reduction of a large number of parameters to a small number of dimensionless numbers [e.g., *Bolster et al.*, 2011]. In the cases under consideration, the driving forces for film drainage of bare viscous bubbles are gravitational and surface tension forces, whereas the resisting force is due to viscosity [*Debrégeas et al.*, 1998]. We will show subsequently why our laboratory experiments are dynamically similar to gravitationally dominated, as well as surface tension-dominated interbubble film drainage in magmas.

3.2.1. Reynolds Number

[24] Inertial forces during film drainage of stagnant bubbles, that is in the absence of an external flow, can be neglected if the Reynolds number, $Re = \rho UL/\eta \ll 1$. Here, Re represents the film Reynolds number, which is the ratio of inertial to viscous forces associated with the flow at the scale of the liquid film, where U is the characteristic velocity and L is the characteristic length scale. For film drainage surrounding a stationary bubble, $L \sim \delta$ and $U \sim u$.

[25] We find that for all of our experiments $Re \ll 1$, implying that our results are applicable to film drainage in cases where the forces that resist fluid motion are dominated by the viscous force. It can be verified that in silicate melts, ranging from mafic to silicic in composition, gravitational or capillary drainage of melt films under most any realistic scenario will be at $Re \ll 1$ [e.g., *Toramaru*, 1988; *Proussevitch et al.*, 1993; *Manga and Stone*, 1994].

3.2.2. Ohnesorge Number

[26] The Ohnesorge number, $Oh = \eta/\sqrt{2\rho\sigma R}$, represents the ratio of viscous to inertial and capillary forces [e.g., *Ohnesorge*, 1936; *Kočárková et al.*, 2013]. For all of our experiments, $Oh \gg 1$ indicating that viscous forces dominate film drainage.

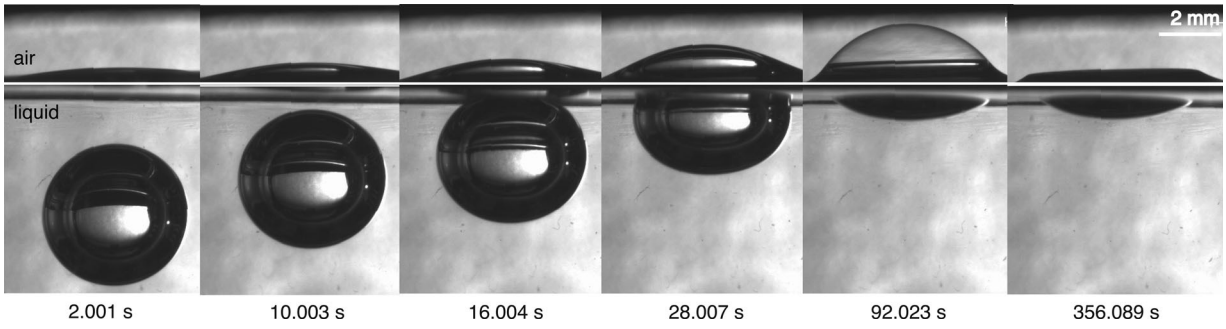

Figure 4. Experimental images of one experiment starting with (left) the bubble approaching the free interface through film drainage and finally (right) coalescence, that is film rupture.

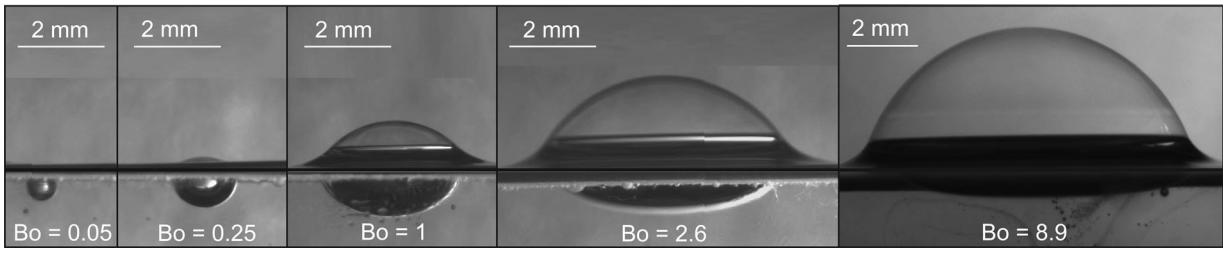

Figure 5. Images showing bubble shapes for different Bond numbers, *Bo*. At $Bo < 0.25$ surface tension forces dominate over gravitational forces, surface area is minimized and the bubble has a spherical shape. At $Bo > 0.25$, gravitational forces dominate and the bubble is no longer spherical in shape. Note that in some images the edges of the flow cell make the liquid interface appear "dirty," which is not the case.

Consistent with previous work [e.g., *Kočárková et al*., 2013, and references therein], we find no dependence of our results on the Ohnesorge number.

3.2.3. Bond Number

[27] The transition between capillary and gravitational film drainage occurs at $R \approx \lambda$. At this transition $t_c = t_g$, so that from equations (6) and (9)

$$\frac{C_g}{C_c} = \frac{\Delta\rho g R^2}{\sigma}. \tag{10}$$

[28] The term on the right-hand side of equation (10) is conventionally defined as the Bond number [e.g., *Stone*, 1994],

$$Bo = \frac{\Delta\rho g R^2}{\sigma}. \tag{11}$$

[29] At $Bo \gg 1$, it is expected that gravitational forces dominate film drainage, whereas for $Bo \ll 1$ surface tension forces are expected to be dominant [e.g., *Proussevitch et al*., 1993; *Stone*, 1994; *Pigeonneau and Sellier*, 2011]. As discussed in detail in section 4, our experimental results show that the transition from capillary to gravitation film drainage occurs at $Bo_t = C_c/C_g = 0.25$, which corresponds to $R = \lambda/2$. Accordingly, bubble shapes change from near spherical at $Bo < 0.25$ to hemispherical at $Bo > 0.25$ (Figure 5) [e.g., *Pigeonneau and Sellier*, 2011]. By varying bubble radii, our experiments spanned the full range of dynamical behavior, from $Bo \ll 1$ to $Bo \gg 1$ (Table 1). This allows us to obtain a self-consistent scaling for film drainage for both capillary-dominated and gravity-dominated film drainage.

3.3. Geometric Similarity

[30] The coalescence of bubbles suspended in viscous liquids, if not caused by deformation due to bulk flow of the suspension, is the consequence of the thinning of interbubble liquid films. It can be caused by either bubble growth, gravitational forces, capillary forces, or some combination thereof. Here, we discuss why and how our experiments with single bubbles can provide constraints on interbubble film drainage, by gravitational or capillary forces, in liquids containing many closely spaced bubbles, as in vesicular magmas.

[31] The geometric constraints of packing a large volume fraction of bubbles into a given volume of melt, require some degree of bubble deformation, relative to an ideal spherical shape [e.g., *Princen et al*., 1980]. Because the Laplace pressure is greater for smaller bubbles than for larger ones, the latter deform more readily than smaller bubbles as they impinge upon one another. The resultant arrangement is often one where smaller bubbles protrude into larger ones. The resultant interbubble films are not flat or of uniform thickness, but of concave/convex shape and thicken toward plateau borders (Figures 1c–1e) [e.g., *Proussevitch et al*., 1993; *Gaonac'h et al*., 1996; *Klug and Cashman*, 1996; *Polacci et al*., 2001; *Klug et al*., 2002; *Rust and Manga*, 2002; *Rust and Cashman*, 2004; *Giachetti et al*., 2010; *Shea et al*., 2010; *Castro et al*., 2012].

[32] Regardless of the detailed geometry, film drainage is a consequence of liquid flow within the film, caused by a gradient in liquid pressure toward the plateau borders [e.g., *Proussevitch et al*., 1993]. In the absence of externally applied deformation, for example, due to magma flow, and neglecting bubble growth, this pressure gradient will be a consequence of capillary and gravitational forces. If the dominant force is due to gravity ($Bo > 0.25$), and irrespective of the precise orientation of the interbubble film relative to the center of gravity, there will be an average pressure gradient of $\Delta\rho g$ within the suspension. This

Table 1. Experimental Parameters

	Parameter	Symbol	Value	Unit
PDMS[a]	Viscosity	η	10–1000	Pa s
	Density	ρ	971–977	kg m^{-3}
	Surface tension	σ	21.2–21.6	mN m^{-1}
	Initial film thickness[b]	δ_0	10–100	μm
	Final film thickness[c]	δ_f	0.1	μm

[a]Includes our experiments presented herein, as well as some experiments by *Kočárková* [2012].

[b]As described in section 4.3.2, the initial film thickness, δ_0, was measured from the bubble images when the bubble became stagnant (Figure 3).

[c]The film thickness at the time of rupture, δ_f, was measured as described in section 4.3.2 and is consistent with the values determined by *Debrégeas et al*. [1998] and *Kočárková* [2012].

pressure gradient causes downward flow within the plateau borders and flow toward the plateau borders within the interbubble films [*Proussevitch et al*., 1993].

[33] If, on the other hand, the dominant force is due to surface tension ($Bo < 0.25$), then the dominant pressure gradients within the interbubble film arise because of changes in the radius of curvature of the film's bounding surface. Surface tension requires a pressure jump across the liquid-gas interface, equal to the value of surface tension divided by the local radius of curvature, $2\sigma/R_c$. Because the gas pressure inside the bubble is essentially uniform, changes in capillary pressure along the liquid-gas interface require lateral pressure gradients within the film itself. Typically, the radius of curvature is smallest in the vicinity of plateau borders, as illustrated in Figures 1b–1e and also in a wide range of publications focused on vesicles in pyroclasts [e.g., *Klug and Cashman*, 1994; *Klug et al*., 2002; *Formenti and Druitt*, 2003; *Gurioli et al*., 2005; *Adams et al*., 2006; *Degruyter et al*., 2010; *Giachetti et al*., 2010; *Houghton et al*., 1998; *Baker et al*., 2012]. Therefore, the liquid pressure within the interbubble film is smallest near the plateau borders, resulting in capillary flow from the interbubble films toward the plateau borders.

[34] Although our experiments comprise a single bubble at the surface of a larger volume of liquid, the liquid film that surrounds our bubble is subjected to the same average gravitational pressure gradient $\Delta\rho g$ as the liquid comprising an interbubble film that is located somewhere within a bubbly suspension. Similarly, capillary stresses, in both our experiments and bubble suspension, scale as the ratio of surface tension to bubble radius, σ/R. Figures 1c–1f show that in both magmas and our experiments there is a change in the radius of curvature that results in lateral pressure gradients within the film. Although, in detail there may be small geometric differences between our experiments and bubbles in magma, which, for the same Bond number, may result in small differences between film drainage times. However, because the overall force balance remains unaffected, our experiments provide to first order a viable analog to interbubble film drainage in vesicular magmas, assuming that external deformation or bubble growth are negligible.

4. Results

4.1. Film Drainage in PDMS

[35] The drainage times, t_d, of the liquid film surrounding air bubbles in PDMS fluid are shown as a function of R in Figure 6a. For a given viscosity, the value of t_d increases with R until there is a transition in the dynamics of film drainage and t_d decreases with R. This inflection in the trend of t_d versus R represents the transition between capillary and gravitational film drainage, at $R = \lambda/2 = 0.75$ mm and $Bo = 0.25$.

[36] A graph of the dimensionless drainage time t_d/t_g versus Bo is shown in Figure 6b. It demonstrates that the drainage time for all experiments with $Bo \geq 0.25$ can be predicted by equation (6), with $t_d/t_g \approx 1$ for $C_g = 5$. We also show that the values of t_d/t_g determined from the published results of *Debrégeas et al*. [1998] and *Kočárková* [2012] (open circles) overlap with our results and do not show a dependence of C_g on Bond number, which is consistent with previous results [*Kočárková et al*., 2013].

[37] Because our experiments span 2 orders of magnitude on either side of $Bo = 0.25$, we are also able to obtain an empirical relation for the capillary drainage time of bare viscous bubbles. We find that for $Bo < 0.25$, a value of $C_c = 20$ in equation (9) provides a good estimate of capillary drainage time, so that $t_c/t_d \approx 1$ (Figure 6c).

[38] It should be noted that equation (1) does not provide an adequate fit to most of our experimental results. This is demonstrated in Figure 7, which compares measured to predicted values of drainage time. While equations (6) and (9) provide a good match to observed values, equation (1) with $n = 2$, as frequently used for film drainage in magmas [e.g., *Cashman et al*., 1994; *Klug and Cashman*, 1996; *Mangan and Cashman*, 1996; *Cruz and Chouet*, 1997; *Herd and Pinkerton*, 1997; *Navon and Lyakhovsky*, 1998; *Castro et al*.,

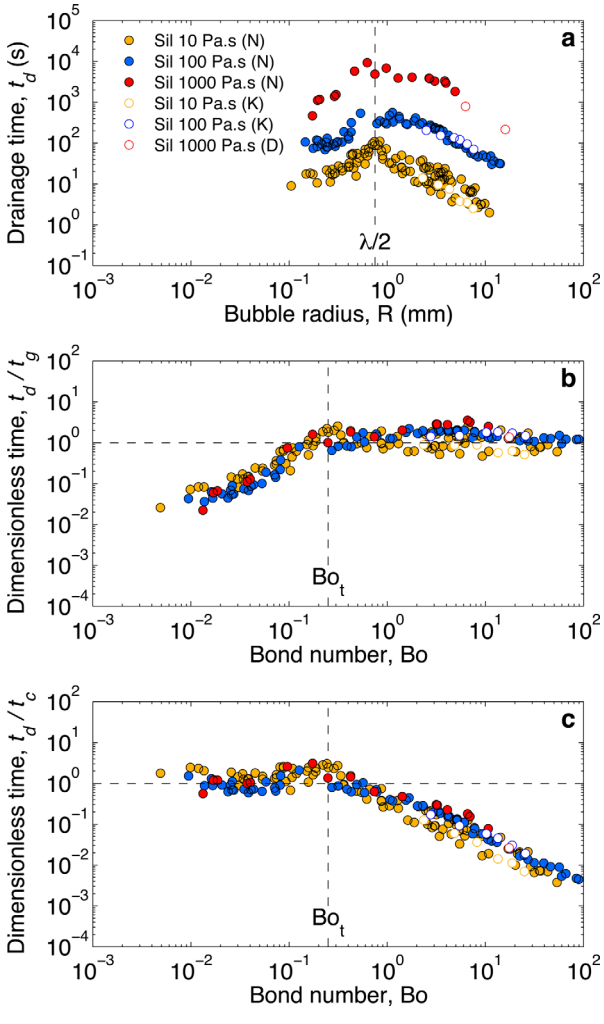

Figure 6. (a) Measured film drainage time, t_d, versus bubble radius, R. Filled circles are experiments from this study using PDMS fluids. Open circles are PDMS experiments by *Debrégeas et al*. [1998] and *Kočárková* [2012]. The transition from capillary drainage to gravitational film drainage occurs at half of the capillary length, $\lambda/2 \approx 0.75$ mm. (b) The same experiments with t_d normalized to the gravitational drainage time, t_g. At $Bo > 0.25$ a value of $t_d/t_g \sim 1$ indicates that equation (6) provides a good estimate for $t_{d,Bo>0.25}$. (c) The same experiments with drainage time, t_d, normalized to the capillary drainage time, t_c. At $Bo < 0.25$, the experimental drainage time also has a value of $t_d/t_c \sim 1$, indicating that equation (9) provides a good estimate for $t_{d,Bo<0.25}$.

2012], overestimates drainage times by up to 8 or 9 orders of magnitude. Even for very small values of the poorly constrained parameter n, only part of the full data set can be matched.

4.2. Film Drainage in Silicate Melts

4.2.1. Observed and Predicted Drainage Times

[39] Figure 7 demonstrates that our scaling relations obtained from film drainage in PDMS also predict film drainage in silicate melts with reasonable accuracy. For silicate melts, *Kočárková et al*. [2013] suggest a modest dependence of C_g on Bond number near the transition to capillary drainage, with the reason for such a dependence remaining unresolved. We find that a Bond number dependent C_g, as suggested by *Kočárková et al*. [2013], does not improve the fit compared to $C_g = 5$. Although no empirical values of t_c currently exist for silicate melts, the fact that gravitational film drainage in silicate melts is consistent with "bare" viscous films suggests that film drainage times in silicate melts at small Bond numbers can be assessed using equation (9).

4.2.2. Surface Tension

[40] Surface tension in the PDMS experiments is almost constant and differs from the silicate melt experiments of *Kočárková* [2012] by only a factor of 1.5 (Table 1). It is therefore important to ascertain that our results have dynamic similarity to natural silicate melts, where the variability in surface tension may only be approximately 1 order of magnitude [e.g., *Walker and Mullins*, 1981; *Bagdassarov et al*., 2000; *Mangan and Sisson*, 2005; *Gardner and Ketcham*, 2011; *Gardner*, 2012; *Kočárková*, 2012], with surface tension in our experimental liquids falling at the lower end of this range. Surface tension affects the dynamics of film drainage through the aforementioned force balances (equation (10), section 3.2). In our experiments, surface tension forces vary by orders of magnitude, from 10^{-5} N to 10^{-2} N, exceeding the range in surface tension forces achievable by reasonable variations in surface tension alone, for either analog fluids or silicate melts. Consequently, our experiments span a wide range of dynamic behavior with the ratio of gravitational to capillary forces ranging from $Bo \ll 1$ to $Bo \gg 1$ (Figure 6).

4.2.3. Viscosity

[41] Because the viscosity of natural silicate melts can exceed the viscosities of our PDMS fluids, the extrapolation of our results to magmatic systems requires dynamic similarity. The liquid viscosity in our experiments ranged from 10 to 10^3 Pa s, within the range of mafic to intermediate magmas [e.g., *Giordano et al*., 2008; *Hui and Zhang*, 2007]. Silicic melts, especially at low water content and low temperature can have viscosities that are substantially larger [e.g., *Hui and Zhang*, 2007], resulting in proportionally smaller velocities (equations (3) and (7)) and hence longer drainage times. The film Reynolds number $\ll 1$ for even the least viscous magmas, implying that the force balance is dominated by viscous stresses in both our PDMS

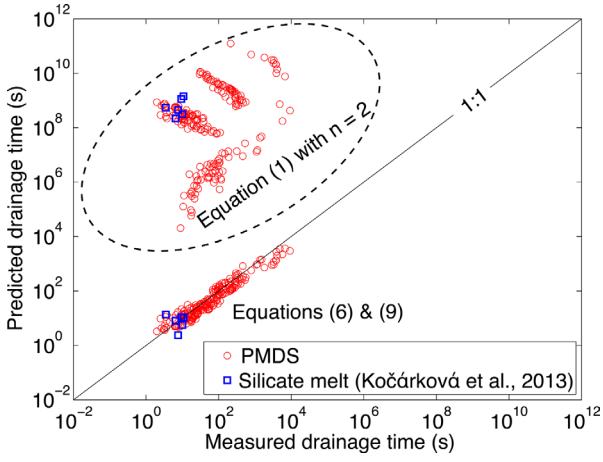

Figure 7. Observed versus predicted film drainage times. Red circles are PDMS experimental data and blue squares are silicate melt data. Experiments plotted within the dashed ellipse have predicted drainage time calculated using equation (1) with $n = 2$ and overpredict drainage times by up to 9 orders of magnitude. Experiments plotted along the 1:1 line have predicted drainage times calculated using equations (6) and (9). Drainage times for silicate melt experiments of *Kočárková et al*. [2013] are shown as blue squares, indicating that equation (6) also predicts film drainage in silicate melt reasonably well. The silicate melts had compositions of 72.3% SiO_2, 13.5% Na_2O, 9.6% CaO, 4% MgO, and 0.6% Al_2O_3, as well as 61.8% SiO_2, 12.6% Na_2O, 0.5% CaO, 9.4% K_2O, 7.6% MgO, and 8.1% Al_2O_3. Corresponding viscosities were 64 and 154 Pa s, densities 2344 and 2318 kg m^{-3}, and surface tension 0.322 and 0.303 N m^{-1}, respectively.

experiments and magmas across the full spectrum of naturally occurring compositions, temperatures, and water contents. As already discussed in section 3.2.2, a dependence on the Ohnesorge number is also not expected. Consequently, our empirical results should be dynamically similar to gravitational and capillary film drainage in magmas ranging from basalt to water-poor rhyolite, in the absence of crystals or other stabilizing impurities, as well as bubble growth or shear deformation.

4.2.4. Interface Mobility

[42] The flow during the drainage of interbubble films depends strongly on the nature of the interfaces between the liquid film and the surrounding gas phase. In many applications, it is desirable to inhibit or slow the drainage of interbubble films, thereby creating a more stable suspension or foam. This is usually achieved by adding surfactants, which, among other things, limit the mobility of the film interfaces. Consequently, liquid flow within the film is similar to flow in a vary narrow gap, bounded by two rigid walls. The flow velocity at each interface approaches zero, making the interface immobile, that is a no-slip boundary (Figure 2a). In this case, equation (1) should be used to estimate the film drainage time, as it is derived using no-slip boundary conditions [*Charles and Mason*, 1960; *Hartland*, 1970; *Ivanov and Traykov*, 1976]. If, on the other hand, there are no impurities at the film interface, the flow velocity is the same at the interface as in the interior (Figure 2b). The interfaces of such a "bare" film are therefore fully mobile. Drainage times of liquid films with such free-slip boundaries are given by equations (6) and (9) [*Debrégeas et al*., 1998; *van der Schaaf and Beerkens*, 2006].

[43] Figure 7 demonstrates that in the absence of crystals or other impurities film drainage times in silicate melts are consistent with fully mobile interfaces. In the absence of crystals or other impurities that may stabilize interbubble films, equations (6) and (9) should be used to predict film drainage times in silicate melts, because calculations based on equation (1) will invariably result in vast overpredictions of drainage times.

4.3. Measurement Errors

4.3.1. Drainage Time

[44] For all experiments, the standard deviation in measured bubble radii, R, is less than 1%. The resultant error bars for R and Bo are smaller than the size of symbols used to present the experimental data (Figures 6 and 7). The experiments covered a range of t_d from approximately 1–5000 s. Figure 3 illustrates the method by which t_d was measured from the time-lapse bubble images. From repeat measurements of t_d on individual samples, we estimated the standard deviation of t_d measurements scaled as $0.25t_d^{2/3}$, which is also smaller than the size of the data symbols.

4.3.2. Film Thickness

[45] Some degree of uncertainty is also associated with the initial and final film thickness, δ_0 and δ_f, respectively. They affect the predicted drainage time (equations (6) and (9)) through the value of $\ln(\delta_0/\delta_f)$. We measured initial film thickness (on the order of hundred's of micrometers) using high-resolution digital images of the bubbles and surrounding films that allowed us to measure δ_0 with an accuracy within 5%, with values ranging from $\sim 10^{-5}$ m to $\sim 10^{-4}$ m. These values are not dissimilar to the maximum thickness of interbubble films observed in some natural volcanic samples [e.g., *Gaonac'h et al*., 1996; *Klug and Cashman*, 1996; *Navon and Lyakhovsky*, 1998; *Formenti and Druitt*, 2003; *Burgisser and Gardner*, 2005;

Polacci et al., 2006; *Bai et al.*, 2008; *Giachetti et al.*, 2010, 2011; *Shea et al.*, 2010].

[46] The critical film thickness prior to the time of rupture was determined from the light reflectance of the film across a spectrum of wavelengths, using instrumentation provided by Filmetrics Incorporated. The method uses an iterative procedure to constrain film thickness and optical parameters from the spectral reflectance measurements. The spot size of these measurements is 200 μm, resulting in a spatially averaged film thickness across the measurement area. The measured values of δ_f are typically of the order of 10^{-7} m (Figure 8). This is consistent with theoretical predictions [e.g., *Sheludko*, 1966; *Coons et al.*, 2003] and also observations of minimum film thicknesses in natural silicate melts (Figure 8) [*Klug and Cashman*, 1996; *Debrégeas et al.*, 1998; *Navon and Lyakhovsky*, 1998; *Burgisser and Gardner*, 2005; *Castro et al.*, 2012; *Kočárková*, 2012]. From repeat measurements, the error in δ_f is estimated to be within few percent of the measured value. In contrast to films with immobile interfaces where drainage time scales as δ_f^{-2} (equation (1)), our predicted drainage times depend on ln (δ_0/δ_f). Consequently, the uncertainty in drainage time predictions due to measurement errors in δ_0 and δ_f is less than a factor of approximately 2 and does not significantly bias our results.

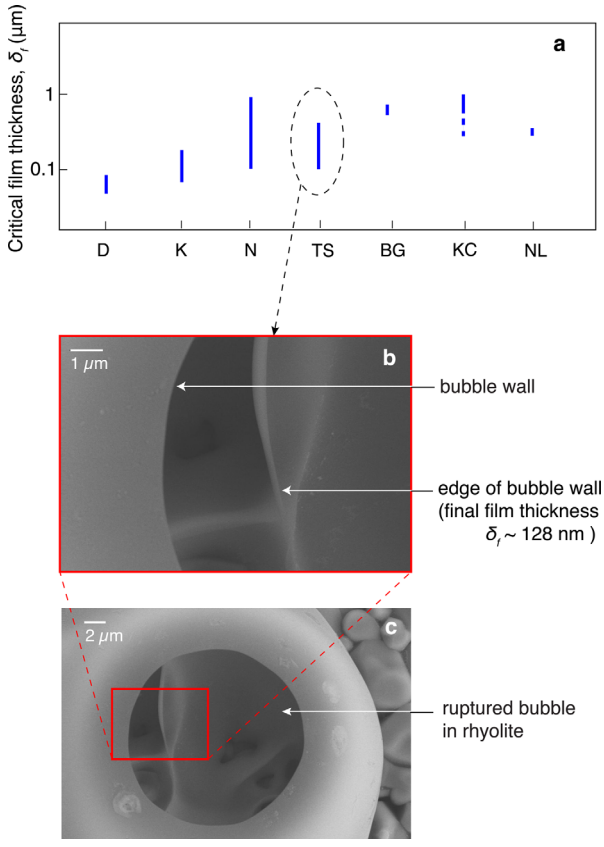

Figure 8. (a) Compilation of critical film thickness measurements. The new PDMS experiments presented herein are labeled as "N," those by *Debrégeas et al.* [1998] as "D," and PDMS and silicate melt experiments by *Kočárková et al.* [2013] combined as "K." Film thickness estimates from SEM images of natural samples are labeled as "KC" [*Klug and Cashman*, 1996], "NL" [*Navon and Lyakhovsky*, 1998], and "BG" [*Burgisser and Gardner*, 2005]. (b) High-resolution SEM image of ruptured bubble wall in natural rhyolite produced in thermal spray vesiculation experiments [*Qu et al.*, 2007; *Qu and Gouldstone*, 2008], showing that ruptured bubble walls are approximately 0.1 μm in thickness (labeled as "TS"). (c) SEM image at higher resolution, showing the ruptured bubble.

5. Implications for Magmatic Systems

[47] Bubble coalescence in magmatic systems often involve ascent-driven magma decompression and shear deformation [e.g., *Sparks*, 1978; *Toramaru*, 1988; *Proussevitch et al.*, 1993; *Cashman et al.*, 1994; *Mader et al.*, 1994; *Klug and Cashman*, 1996; *Larsen et al.*, 2004; *Burgisser and Gardner*, 2005; *Okumura et al.*, 2006; *Moitra et al.*, 2013]. To assess the conditions under which these processes significantly increase the rates of bubble coalescence requires constraints on the time scales of interbubble film drainage in the absence of bubble growth or external deformation. In other words, capillary and gravitational film drainage give a lower bound on coalescence rates.

5.1. Predicted Film Drainage Time in Silicate Melts

[48] Film drainage rates depend on bubble size, as well as material properties, such as viscosity and surface tension. The typical vesicle size ranges between 10^{-6} m and 10^{-2} m for silicic pumices [e.g., *Toramaru*, 1990; *Klug and Cashman*, 1994; *Gaonac'h et al.*, 1996; *Blower et al.*, 2003; *Klug et al.*, 2002; *Rust and Cashman*, 2004; Gaonac'h et al., 2005; *Giachetti et al.*, 2010; *Shea et al.*, 2010] and even larger in basaltic scoria [e.g., *Mangan et al.*, 1993; *Mangan and Cashman*, 1996; *Vergniolle*, 1986; *Lautze and Houghton*, 2007; *Polacci et al.*, 2008, 2009]. Surface tension for natural silicate melts ranges within an order of magnitude, from 0.03 to 0.3 N m^{-1} [e.g., *Epel'baum et al.*, 1973; *Murase and McBirney*, 1973; *Khitarov et al.*, 1979; *Walker and Mullins*, 1981; *Taniguchi*, 1988; *Bagdassarov et al.*, 2000;

Mangan and Sisson, 2005; *Gardner and Ketcham*, 2011; *Gardner*, 2012]. In contrast, melt viscosity can vary by many orders of magnitude [e.g., *Hess and Dingwell*, 1996; *Hui and Zhang*, 2007].

[49] For the range of feasible parameters discussed above, we estimate the drainage time in both capillary and gravitational regimes using equations (6) and (9). The results are shown in Figure 9 and indicate that film drainage times for adjacent bubbles in basaltic melts, even in the absence of bubble growth or external deformation, will be 10 s of seconds or less. In intermediate and silicic melts, film drainage times are considerably larger, with up to $\sim 10^9$ s in dry rhyolitic melts.

5.2. Postfragmentation Coalescence in Pyroclasts

[50] Bubble coalescence may result in magma permeability with ensuing implications for open-system magma degassing and magma fragmentation [e.g., *Westrich and Eichelberger*, 1994; *Klug and Cashman*, 1996; *Saar and Manga*, 1999; *Blower*, 2001; *Burgisser and Gardner*, 2005; *Okumura et al.*, 2006; *Wright et al.*, 2006; *Mueller et al.*, 2008; *Namiki and Manga*, 2008; *Okumura et al.*, 2008; *Wright et al.*, 2009; *Rust and Cashman*, 2011; *Castro et al.*, 2012; *Namiki*, 2012]. Because magma ascent conditions are inferred from measured textural characteristics and permeabilities in pyroclasts, it is important to assess the extent of bubble coalescence after magma fragmentation, and thus, the likelihood that measured values are significantly different from conditions prior to fragmentation.

[51] During the time interval between magma fragmentation and quenching, when shear deformation may no longer be the dominant processes and when characteristic length scales for permeable gas flow are of the order of centimeters, bubble growth may be negligible, because permeable gas loss may efficiently dissipating gas pressure [*Rust and Cashman*, 2011; *Gonnermann and Houghton*, 2012]. If this is the case, postfragmentation bubble coalescence rates can be estimated from estimates for interbubble film drainage rates. Thus, if postfragmentation coalescence can be shown to be negligible, then pyroclast textural characteristics, such vesicle size distributions, as well as permeabilities likely provide a reliable record of prefragmentation conditions.

[52] Cooling times of pyroclasts have been estimated to be of the order of 10–100 s [e.g., *Thomas and Sparks*, 1992; *Hort and Gardner*, 1998]. Figure 9 indicates that film drainage times may only be of similar or shorter duration as cooling times in relatively water-rich intermediate melts. Consequently, it is unlikely that there is sufficient interbubble film drainage in pyroclasts from explosive intermediate to silicic magmas to significantly change pyroclast vesicle size distributions and permeability after magma fragmentation.

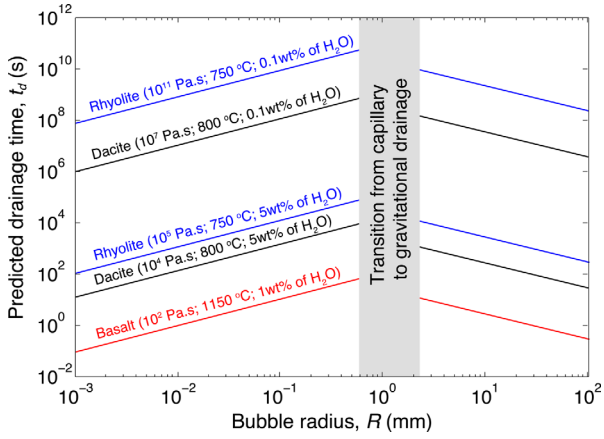

Figure 9. Illustrative predictions of film drainage time (in the absence of bubble growth or shear deformation) in basalt (red), dacite (black), and rhyolite (blue) melts using viscosities from *Hui and Zhang* [2007] at the indicated temperatures and water contents. At small radii, where film drainage is dominated by capillary drainage, predicted drainage times are plotted at a surface tension of $\sigma = 0.1$ N m^{-1}, whereas gravitationally dominated film drainage is independent of surface tension.

6. Conclusions

[53] We presented laboratory experiments wherein we measured the lifetime of stationary air bubbles suspended beneath the free surface of surfactant-free PDMS liquids. To ensure dynamic similarity to magmatic systems, all experiments were at small Reynolds numbers ($Re \ll 1$) and cover a wide range of Bond number, $10^{-3} \leq Bo \leq 10^2$, with the transition between capillary and gravitational drainage corresponding to a Bond number of 0.25. Our results are consistent with similar experiments in PDMS and in silicate melts. They provide predictions of film drainage times that can be applied to bubbles in magma, if shear deformation and bubble growth are negligible, and if interbubble films are not stabilized, for example, by the presence of abundant microlites. Overall, our results indicate that textural characteristics and permeabilities of pyroclasts from intermediate to silicic magmas may preserve prefragmentation

conditions. Furthermore, film drainage times in magmas are likely orders of magnitude shorter than previous estimates that are based on formulations for liquid films with immobile interfaces.

Acknowledgments

[54] We thank T. Giachetti, as well as K. Cashman and the other anonymous reviewer for constructive comments. This material is based upon work supported by the National Science Foundation under grants NSF EAR-1019872, NSF EAR-1250451, and NSF IDR-1015069. Any opinions, findings, and conclusions or recommendations expressed in this material are those of the authors and do not necessarily reflect the views of the National Science Foundation.

References

Abid, S., and A. K. Chesters (1994), The drainage and rupture of partially mobile films between colliding drops at constant approach velocity, *Int. J. Multiphase Flow*, *20*, 613–629.

Adams, N. K., B. F. Houghton, S. A. Fagents, and W. Hildreth (2006), The transition from explosive to effusive eruptive regime: The example of the 1912 Novarupta eruption, Alaska, *Geol. Soc. Am. Bull.*, *118*, 620–634.

Alatorre-Ibargüengoitia, M. A., B. Scheu, D. B. Dingwell, H. Delgado-Granados, and J. Taddeucci (2010), Energy consumption by magmatic fragmentation and pyroclast ejection during Vulcanian eruptions, *Earth Planet. Sci. Lett.*, *291*, 60–69, doi:10.1016/j.epsl.2009.12.051.

Alidibirov, M., and D. B. Dingwell (2000), Three fragmentation mechanisms for highly viscous magma under rapid decompression, *J. Volcanol. Geotherm. Res.*, *100*, 413–421, doi:10.1016/S0377-0273(00)00149-9.

Bagdassarov, N. S., A. Dorfman, and D. B. Dingwell (2000), Effect of alkalis, phosphorus, and water on the surface tension of haplogranite melt, *Am. Mineral.*, *85*, 33–40.

Bai, L., D. R. Baker, and M. Rivers (2008), Experimental study of bubble growth in Stromboli basalt melts at 1 atm, *Earth Planet. Sci. Lett.*, *267*, 533–547, doi:10.1016/j.epsl.2007.11.063.

Baker, D. R., L. Mancini, M. Polacci, M. D. Higgins, G. A. R. Gualda, R. J. Hill, and M. L. Rivers (2012), An introduction to the application of X-ray microtomography to the three-dimensional study of igneous rocks, *Lithos*, *148*, 262–276.

Blower, J. D. (2001), Factors controlling permeability—Porosity relationships in magma, *Bull. Volcanol.*, *63*, 497–504.

Blower, J. D., J. P. Keating, H. M. Mader, and J. C. Phillips (2003), The evolution of bubble size distributions in volcanic eruptions, *J. Volcanol. Geotherm. Res.*, *120*, 1–23, doi:10.1016/S0377-0273(02)00404-3.

Blundy, J., and K. V. Cashman (2008), Petrologic reconstruction of magmatic system variables and processes, *Rev. Miner. Geochem.*, *69*, 179–239.

Bolster, D., R. E. Hershberger, and R. J. Donnelly (2011), Dynamic similarity, the dimensionless science, *Phys. Today*, *64*, 42–47.

Burgisser, A., and J. E. Gardner (2005), Experimental constraints on degassing and permeability in volcanic conduit flow, *Bull. Volcanol.*, *67*, 42–56.

Cashman, K. V., and M. Mangan (1994), Physical aspects of magmatic degassing. II. Constraints on vesiculation processes from textural studies of eruption product, *Rev. Mineral.*, *30*, 477–478.

Cashman, K. V., M. Mangan, and S. Newman (1994), Surface degassing and modifications to vesicle size distributions in active basalt flows, *J. Volcanol. Geotherm. Res.*, *61*, 45–68, doi:10.1016/0377-0273(94)00015-8.

Castro, J. M., A. Burgisser, C. I. Schipper, and S. Mancini (2012), Mechanisms of bubble coalescence in silicic magmas, *Bull. Volcanol.*, *74*, 2339–2352.

Chan, D. Y. C., E. Klaseboer, and R. Manica (2011), Film drainage and coalescence between deformable drops and bubbles, *Soft Matter*, *7*, 2235–2264.

Charles, G. E., and S. G. Mason (1960), The coalescence of liquid drops with flat liquid/liquid interfaces, *J. Colloid Sci.*, *15*, 236–267.

Chesters, A. K. (1988), Drainage of partially mobile films between colliding drops: A first order model, *Proc. Euromech*, Int. Conf. on Turbulent Two Phase Flow Systems, Toulouse, France, p.234.

Chesters, A. K., and G. Hofman (1982), Bubble coalescence in pure liquids, *Appl. Sci. Res.*, *38*, 353–361.

Coons, J. E., P. J. Halley, S. A. McGlashan, and T. Tran-Cong (2003), A review of drainage and spontaneous rupture in free standing thin films with tangentially immobile interfaces, *Adv. Colloid Interface Sci.*, *105*, 3–62.

Cruz, F. G., and B. A. Chouet (1997), Long-period events, the most characteristic seismicity accompanying the emplacement and extrusion of a lava dome in Galeras Volcano, Colombia, in 1991, *J. Volcanol. Geotherm. Res.*, *77*, 121–158, doi:10.1016/S0377-0273(96)00091-1.

Davis, S. S., and A. Smith (1976), Stability of hydrocarbon oil droplets at surfactant-oil interface, *Coll. Polymer Sci.*, *254*, 82–99.

Debrégeas, G., P. G. de Gennes, and F. B. Wyart (1998), The life and death of "bare" viscous bubbles, *Science*, *279*, 1704–1707.

Degruyter, W., O. Bachmann, and A. Burgisser (2010), Controls on magma permeability in the volcanic conduit during the climatic phase of the Kos Plateau Tuff eruption (Aegean Arc), *Bull. Volcanol.*, *72*, 63–74.

Eichelberger, J. C., C. R. Carrigan, H. R. Westrich, and R. H. Price (1986), Non-explosive silicic volcanism, *Nature*, *323*, 598–602.

Epel'baum, M. B., I. V. Babashov, and T. P. Salova (1973), Temperatures and pressures, *Geochem. Int.*, *10*, 343–345.

Formenti, Y., and T. H. Druitt (2003), Vesicle connectivity in pyroclasts and implications for the fluidisation of fountain-collapse pyroclastic flows, Montserrat (West Indies), *Earth Planet. Sci. Lett.*, *214*, 561–574, doi:10.1016/S0012–821X(03)00386-8.

Gaonac'h, H., J. Stix, and S. Lovejoy (1996), Scaling effects on vesicle shape, size and heterogeneity of lavas from Mount Etna, *J. Volcanol. Geotherm. Res.*, *74*, 131–153, doi:10.1016/S0377-0273(96)00045-5.

Gaonac'h, H., S. Lovejoy, and D. Scherzter (2005), Scaling vesicle size distributions and volcanic eruptions, *Bull. Volcanol.*, *67*, 350–357.

Gardner, J. E. (2007), Bubble coalescence in rhyolitic melts during decompression from high pressure, *J. Volcanol. Geotherm. Res.*, *166*, 161–176, doi:10.1016/j.jvolgeores.2007.07.006.

Gardner, J. E. (2012), Surface tension and bubble nucleation in phonolite magmas, *Geochim. Cosmochim. Acta*, *76*, 93–102.

Gardner, J. E., and R. A. Ketcham (2011), Bubble nucleation in rhyolite and dacite melts: Temperature dependence of surface tension, *Contrib. Mineral. Petrol.*, *162*, 929–943.

Giachetti, T., T. H. Druit, A. Burgisser, L. Arbaret, and C. Galven (2010), Bubble nucleation, growth and coalescence during the 1997 Vulcanian explosions of Soufriere Hills Volcano, Montserrat, *J. Volcanol. Geotherm. Res.*, *193*, 215–231, doi:10.1016/j.jvolgeores.2010.04.001.

Giachetti, T., A. Burgisser, L. Arbaret, T. H. Druit, and K. Kelfoun (2011), Quantitative textural analysis of Vulcanian pyroclasts (Montserrat) using multi-scale X-ray computed microtomography: Compared with results from 2D image analysis, *Bull. Volcanol.*, *73*, 1295–1309.

Giordano, D., J. K. Russell, and D. B. Dingwell (2008), Viscosity of magmatic liquids: A model, *Earth Planet. Sci. Lett.*, *271*, 123–134, doi:10.1016/j.epsl.2008.03.038.

Gonde, C., C. Martel, M. Pichavanti, and H. Bureau (2011), In-situ bubble vesiculation in silicic magmas, *Am. Mineral.*, *96*, 111–124.

Gonnermann, H. M., and B. F. Houghton (2012), Magma degassing and fragmentation during the Plinian eruption of Novarupta, Alaska, 1912, *Geochem. Geophys. Geosyst.*, *13*, Q10009, doi:10.1029/2012GC004273.

Gonnermann, H. M., and M. Manga (2007), The fluid mechanics inside a volcano, *Annu. Rev. Fluid Mech.*, *39*, 321–356.

Gurioli, L., B. F. Houghton, K. V. Cashman, and R. Cioni (2005), Complex changes in eruption dynamics during the 79 AD eruption of Vesuvius, *Bull. Volcanol.*, *67*, 144–159.

Hartland, S. (1970), The profile of the drainage film between a fluid drop and a deformable fluid- liquid interface, *Chem. Eng. Sci.*, *1*, 67–75.

Herd, R. A., and H. Pinkerton (1997), Bubble coalescence in basaltic lava: Its impact on the evolution of bubble populations, *J. Volcanol. Geotherm. Res.*, *75*, 137–157, doi:10.1016/S0377-0273(96)00039-X.

Hess, K. U., and D. B. Dingwell (1996), Viscosities of hydrous leucogranitic melts: A non-Arrhenian model, *Am. Mineral.*, *81*, 1297–1300.

Hort, M., and J. Gardner (1998), Constraints on cooling and degassing of pumice during Plinian volcanic eruptions based on model calculations, *J. Geophys. Res.*, *105*, 25,981–26,001.

Houghton, B. F., and C. J. N. Wilson (1989), A vesicularity index for pyroclastic deposits, *Bull. Volcanol.*, *51*, 451–462.

Houghton, B. F., R. J. Carey, K. V. Cashman, C. J. N. Wilson, B. J. Hobden, and J. E. Hammer (1998), Diverse patterns of ascent, degassing, and eruption of rhyolite magma during the 1.8 ka Taupo eruption, New Zealand: Evidence from clast vesicularity, *J. Volcanol. Geotherm. Res.*, *105*, 25,981–26,001, doi:10.1016/j.jvolgeores.2010.06.002.

Hui, H., and Y. Zhang (2007), Toward a general viscosity equation for natural anhydrous and hydrous silicate melts, *Geochim. Cosmochim. Acta*, *71*, 403–416.

Ivanov, I. B., and T. T. Traykov (1976), Hydrodynamics of thin liquid films, Rate of thinning of emulsion films from pure liquids, *Int. J. Multiphase Flow*, *2*, 397–410.

Jones, A. F., and S. D. Wilson (1978), The film drainage problem in droplet coalescence, *J. Fluid Mech.*, *87*, 263–288.

Khitarov, N. I., Y. B. Lebedev, A. M. Dorfman, and N. S. Bagdassarov (1979), Effects of temperature, pressure and volatiles on the surface tension of molten basalt, *Geochem. Int.*, *16*, 78–86.

Kline, S. J. (1986), *Similitude and Approximation Theory*, 248 pp., Springer, New York.

Klug, C., and K. V. Cashman (1994), Vesiculation of May 18, 1980 Mount St. Helens magma, *Geology*, *22*, 468–472.

Klug, C., and K. V. Cashman (1996), Permeability development in vesiculating magmas: Implications for fragmentation, *Bull. Volcanol.*, *58*, 87–100.

Klug, C., K. V. Cashman, and C. R. Bacon (2002), Structure and physical characteristics of pumice from climatic eruption of Mt. Mazama (Crater Lake), Oregon, *Bull. Volcanol.*, *64*, 486–501.

Kočárková, H. (2012), Stability of glass foams: Experiments at bubble scale and on vertical film, PhD dissertation, Université Paris - Est, Paris, France.

Kočárková, H., F. Rouyer, and F. Pigeonneau (2013), Film drainage of viscous liquid on top of bare bubble: Influence of the Bond number, *Phys. Fluids*, *1-25*, doi:10.1063/1.4792310.

Koyaguchi, T., and N. Mitani (2005), A theoretical model for fragmentation of viscous bubbly magmas in shock tubes, *J. Geophys. Res.*, *110*, B10202, doi:10.1029/2004JB003513.

Koyaguchi, T., B. Scheu, N. K. Mitani, and O. Melnik (2008), A fragmentation criterion for highly viscous bubbly magmas estimated from shock tube experiments, *J. Volcanol. Geotherm. Res.*, *178*, 58–71, doi:10.1016/j.jvolgeores.2008.02.008.

Larsen, J. F., M. H. Denis, and J. E. Gardner (2004), Experimental study of bubble coalescence in rhyolitic and phonolitic melts, *Geochim. Cosmochim. Acta*, *68*, 333–344.

Lautze, N. C., and B. F. Houghton (2007), Linking variable explosion style and magma textures during 2002 at Stromboli volcano, Italy, *Bull. Volcanol.*, *69*, 445–460.

Lee, J. C., and T. D. Hodgson (1968), Film flow and coalescence—I. Basic relations, film shape and criteria for interface mobility, *Chem. Eng. Sci.*, *23*, 1375–1397.

Llewellin, E. W., and M. Manga (2005), Bubble suspension rheology and implications for conduit-flow, *J. Volcanol. Geotherm. Res.*, *143*, 205–217, doi:10.1016/j.jvolgeores.2004.09.018.

Lovejoy, S., H. Gaonac'h, and D. Schertzer (2004), Bubble distributions and dynamics: The expansion-coalescence equation, *J. Geophys. Res.*, *109*, B11203, doi:10.1029/2003JB002823.

Mader, H. M., M. Zhang, J. C. Phillips, R. S. J. Sparks, B. Sturtevant, and E. Stolper (1994), Experimental simulations of explosive degassing of magma, *Nature*, *372*, 85–88.

Mader, H. M., M. Manga, and T. Koyaguchi (2004), The role of laboratory experiments in volcanology, *J. Volcanol. Geotherm. Res.*, *129*, 1–5, doi:10.1016/S0377-0273(03)00228-2.

Manga, M., and H. A. Stone (1994), Interactions between bubbles in magmas and lavas: Effects on bubble deformation, *J. Volcanol. Geotherm. Res.*, *63*, 267–279, doi:10.1016/0377-0273(94)90079-5.

Manga, M., J. Castro, K. V. Cashman, and M. Loewenberg (1998), Rheology of bubble-bearing magmas, *J. Volcanol. Geotherm. Res.*, *87*, 15–28, doi:10.1016/S0377-0273(98)00091-2.

Mangan, M. T., and K. V. Cashman (1996), The structure of basaltic scoria and reticulite and inferences for vesiculation, foam formation, and fragmentation in lava fountains, *J. Volcanol. Geotherm. Res.*, *73*, 1–18, doi:10.1016/0377-0273(96)00018-2.

Mangan, M. T., and T. Sisson (2005), Evolution of melt-vapor surface tension in silicic volcanic systems: Experiments with hydrous melts, *J. Geophys. Res.*, *110*, B01202, doi:10.1029/2004JB003215.

Mangan, M. T., K. V. Cashman, and S. Newman (1993), Vesiculation of basaltic magma during eruption, *Geology*, *21*, 157–160.

Martula, D. S., T. Hasegawa, D. R. Lloyd, and R. T. Bonnecaze (2000), Coalescence-induced coalescence of inviscid droplets in a viscous fluid, *J. Colloid Sci.*, *232*, 241–253.

Moitra, P., H. M. Gonnermann, B. F. Houghton, and T. Giachetti (2013), Relating vesicle shapes in pyroclasts to eruption styles, *Bull. Volcanol.*, *75*, 1–14.

Mueller, S., B. Scheu, O. Spieler, and D. B. Dingwell (2008), Permeability control on magma fragmentation, *Geology*, *36*, 399–402.

Murase, T., and A. R. McBirney (1973), Properties of some common igneous rocks and their melts at high temperatures, *Geol. Soc. Am. Bull.*, *84*, 3563–3587.

Namiki, A. (2012), An empirical scaling of shear-induced outgassing during magma ascent: Intermittent magma ascent causes effective outgassing, *Earth Planet. Sci. Lett.*, *353–354*, 72–81, doi:10.1016/j.epsl.2012.08.007.

Namiki, A., and M. Manga (2005), Response of a bubble bearing viscoelastic fluid to rapid decompression: Implications for explosive volcanic eruptions, *Earth Planet. Sci. Lett.*, *236*, 269–284, doi:10.1016/j.epsl.2005.02.045.

Namiki, A., and M. Manga (2008), Transition between fragmentation and permeable outgassing of low viscosity magmas, *J. Volcanol. Geotherm. Res.*, *169*, 48–60, doi:10.1016/j.jvolgeores.2007.07.020.

Navon, O., and V. Lyakhovsky (1998), Vesiculation processes in silicic magmas, *Geol. Soc. Spec. Publ. 145*, 27–50.

Ohnesorge, W. (1936), Formation of drops by nozzles and the breakup of liquid jets, *J. App. Math. Mech.*, *16*, 355–358.

Okumura, S., M. Nakamura, and A. Tsuchiyama (2006), Shear-induced bubble coalescence in rhyolitic melts with low vesicularity, *J. Geophys. Res.*, *33*, L20316, doi:10.1029/2006GL027347.

Okumura, S., M. Nakamura, A. Tsuchiyama, T. Nakano, and K. Uesugi (2008), Evolution of bubble microstructure in sheared rhyolite: Formation of a channel-like bubble network, *J. Geophys. Res.*, *113*, B07208, doi:10.1029/2007JB005362.

Oldenziel, G., R. Delfos, and J. Westerweel (2012), Measurements of liquid film thickness for a droplet at a two-fluid interface, *Phys. Fluids*, *24*, 022106.

Pal, R. (2003), Rheology behavior of bubble-bearing magmas, *Earth Planet. Sci. Lett.*, *207*, 165–179, doi:10.1016/S0377-0273(98)00091-2.

Pigeonneau, F., and A. Sellier (2011), Low-Reynolds-number gravity-driven migration and deformation of bubbles near a free surface, *Phys. Fluids*, *23*, 092102.

Polacci, M., P. Papale, and M. Rosi (2001), Textural heterogeneities in pumices from the climatic eruption of Mount Pinatubo, 15 June 1991, and implications for magma ascent dynamics, *Bull. Volcanol.*, *63*, 83–97.

Polacci, M., D. R. Baker, L. Mancini, G. Tromba, and F. Zanini (2006), Three-dimensional investigation of volcanic textures by X-ray microtomography and implications for conduit processes, *Geophys. Res. Lett.*, *33*, L13312, doi:10.1029/2006GL026241.

Polacci, M., D. R. Baker, L. Bai, and L. Mancini (2008), Large vesicles record pathways of degassing at basaltic volcanoes, *Bull. Volcanol.*, *70*, 1023–1029.

Polacci, M., D. R. Baker, L. Mancini, S. Favretto, and R. J. Hill (2009), Vesiculation in magmas from Stromboli and implications for normal Strombolian activity and paroxysmal explosions in basaltic systems, *J. Geophys. Res.*, *114*, B01206, doi:10.1029/2008JB005672.

Princen, H. M. (1963), Shape of a fluid drop at a liquid-liquid interface, *J. Colloid Sci.*, *18*, 178–195.

Princen, H. M., M. P. Aronson, and J. C. Moser (1980), Highly concentrated emulsions. II. Real systems—The effect of film thickness and contact angle on the volume fraction in creamed emulsions, *J. Colloid Interface Sci.*, *75*, 246–270.

Proussevitch, A. A., D. L. Sahagian, and V. A. Kutolin (1993), Stability of foams in silicate melts, *J. Volcanol. Geotherm. Res.*, *59*, 161–178, doi:10.1016/0377-0273(93)90084-5.

Qu, M., and A. Gouldstone (2008), On the role of bubbles in metallic splat nanopores and adhesion, *J. Therm. Spray Technol.*, *17*, 486–595.

Qu, M., Y. Wu, V. Srinivasan, and A. Gouldstone (2007), Observations of nanoporous foam arising from impact and rapid solidification of molten Ni droplets, *Appl. Phys. Lett.*, *90*, 254,101–254,103.

Rust, A., and M. Manga (2002), Bubble shapes and orientations in low Re simple shear flow, *J. Colloid Sci.*, *249*, 476–480.

Rust, A. C., and K. V. Cashman (2004), Permeability of vesicular silicic magma: Inertial and hysteresis effects, *Earth Planet. Sci. Lett.*, *228*, 93–107, doi:10.1016/j.epsl.2004.09.025.

Rust, A. C., and K. V. Cashman (2011), Permeability controls on expansion and size distributions of pyroclasts, *J. Geophys. Res.*, *116*, B11202, doi:10.1029/2011JB008494.

Rutherford, M. J. (2008), Magmas ascent rates, *Rev. Miner. Geochem.*, *69*, 241–271.

Rutherford, M. J., and P. M. Hill (1993), Magmas ascent rates from amphibole breakdown: An experimental study applied to the 1980–1986 Mt. St. Helens eruptions, *J. Geophys. Res.*, *98*, 19,678–19,685, doi:10.1029/93JB01613.

Saar, M. O., and M. Manga (1999), Permeability—Porosity relationship in vesicular basalts, *Geophys. Res. Lett.*, *26*, 111–114, doi:10.1029/1998GL900256.

Shea, T., B. F. Houghton, L. Gurioli, K. V. Cashman, J. E. Hammer, and B. J. Hobden (2010), Textural studies of vesicles in volcanic rocks: An integrated methodology, *J. Volcanol. Geotherm. Res.*, *190*, 271–289, doi:10.1016/j.jvolgeores.2009.12.003.

Sheludko, A. D. (1966), *Colloid Chemistry*, 277 pp., Elsevier, New York.

Sparks, R. S. J. (1978), The dynamics of bubble formation and growth in magmas, *J. Volcanol. Geotherm. Res.*, *3*, 1–37, doi:10.1016/0377-0273(78)90002-1.

Sparks, R. S. J., and S. Brazier (1982), New evidence for degassing processes during explosive eruptions, *Nature*, *295*, 218–220.

Spieler, O., B. Kennedy, U. Kueppers, D. B. Dingwell, B. Scheu, and J. Taddeucci (2004), The fragmentation threshold of pyroclastic rocks, *Earth Planet. Sci. Lett.*, *226*, 139–148, doi:10.1016/j.epsl.2004.07.016.

Stein, D. J., and F. J. Spera (1992), Rheology and microstructure of magmatic emulsions: Theory and experiments, *J. Volcanol. Geotherm. Res.*, *49*, 157–174, doi:10.1016/0377-0273(92)90011-2.

Stone, H. A. (1994), Dynamics of drop deformation and breakup, *Annu. Rev. Fluid Mech.*, *26*, 65–102.

Taniguchi, H. (1988), Surface tension of melts in the system $CaMgSi_2O_6$–$CaAl_2Si_2O_8$ and its structural significance, *Contrib. Mineral. Petrol.*, *100*, 484–489.

Thomas, R. M. E., and R. S. J. Sparks (1992), Cooling of tephra during fallout from eruption columns, *Bull. Volcanol.*, *54*, 542–553.

Toramaru, A. (1988), Formation of propagation pattern in two-phase flow systems with applications to volcanic eruptions, *Geophys. J.*, *95*, 613–623, doi:10.1111/j.1365-246X.1988.tb06707.x.

Toramaru, A. (1989), Vesiculation process and bubble size distribution in ascending magmas with constant velocities, *J. Geophys. Res.*, *94*, 17,523–17,542, doi:10.1029/JB094iB12p17523.

Toramaru, A. (1990), Measurement of bubble size distribution in vesiculated rocks with implications for quantitative estimation of eruption processes, *J. Volcanol. Geotherm. Res.*, *43*, 71–90, doi:10.1016/0377-0273(90)90045-H.

Toramaru, A. (2006), BND (bubble number density) decompression rate meter for explosive volcanic eruptions, *J. Volcanol. Geotherm. Res.*, *154*, 303–316, doi:10.1016/j.jvolgeores.2006.03.027.

Traykov, T. T., E. D. Manev, and I. B. Ivanov (1977), Hydrodynamics of thin liquid films, Experimental investigation of the effect of surfactants on the drainage of emulsion films, *Int. J. Multiphase Flow*, *3*, 485–494.

van der Schaaf, J., and R. G. C. Beerkens (2006), A model for foam formation, stability, and breakdown in glass-melting furnaces, *J. Colloid Interface Sci.*, *295*, 218–229.

Vergniolle, S. (1986), Bubble size distribution in magma chambers and dynamics of basaltic eruptions, *J. Geophys. Res.*, *91*, 12,842–12,860, doi:10.1016/0012–821X(96)00042-8.

Walker, D., and O. Mullins (1981), Surface tension of natural silicate melts from 1,200°–1,500°C and implications for melt structure, *Contrib. Mineral. Petrol.*, *76*, 455–462.

Westrich, H. R., and J. C. Eichelberger (1994), Gas transport and bubble collapse in rhyolitic magma: an experimental approach, *Bull. Volcanol.*, *56*, 447–458.

Whitham, A. G., and R. S. J. Sparks (1986), Pumice, *Bull. Volcanol.*, *48*, 209–223.

Wright, H. M. N., J. J. Roberts, and K. V. Cashman (2006), Permeability of anisotropic tube pumice: Model calculations and measurements, *Geophys. Res. Lett.*, *33*, L17316, doi:10.1029/2006GL027224.

Wright, H. M. N., K. V. Cashman, E. H. Gottesfeld, and J. J. Roberts (2009), Pore structure of volcanic clasts: Measurements of permeability and electrical conductivity, *Earth Planet. Sci. Lett.*, *280*, 93–104, doi:10.1016/j.epsl.2009.01.023.

Yiantsios, S. G., and R. H. Davis (1991), Close approach and deformation of two viscous drops due to gravity and van der waals forces, *J. Colloid Sci.*, *144*, 412–433.